Approximate Nullspace Augmented Finetuning for Robust Vision Transformers

Abstract

Enhancing the robustness of deep learning models, particularly in the realm of vision transformers (ViTs), is crucial for their real-world deployment. In this work, we provide a finetuning approach to enhance the robustness of vision transformers inspired by the concept of nullspace from linear algebra. Our investigation centers on whether a vision transformer can exhibit resilience to input variations akin to the nullspace property in linear mappings, implying that perturbations sampled from this nullspace do not influence the model's output when added to the input. Firstly, we show that for many pretrained ViTs, a non-trivial nullspace exists due to the presence of the patch embedding layer. Secondly, as nullspace is a concept associated with linear algebra, we demonstrate that it is possible to synthesize approximate nullspace elements for the non-linear blocks of ViTs employing an optimisation strategy. Finally, we propose a fine-tuning strategy for ViTs wherein we augment the training data with synthesized approximate nullspace noise. After finetuning, we find that the model demonstrates robustness to adversarial and natural image perbutations alike.

1 INTRODUCTION

The field of computer vision has experienced significant advances, marked by the emergence of Vision Transformers (ViTs) [Dosovitskiy et al., 2021] as a notable milestone. Following this advancement, a series of architectural refinements have been explored [Ali et al., 2021, Li et al., 2022, Liu et al., 2021], paving the way for the development of vision foundation models [Kirillov et al., 2023, Zou et al., 2023] through the scaling up of both the model and dataset. Despite these strides, robustness continues to be a pivotal concern for their practical deployment, as they exhibit fragility in the face of imperceptible (adversarial) and perceptible perturbations.

Adversarial samples are generated by adding imperceptible noises to the input, aiming to cause the model to produce incorrect and overly confident predictions [Goodfellow et al., 2015, Moosavi-Dezfooli et al., 2016, Nguyen et al., 2015]. Perceptible perturbations are artifacts that arise from various operations, such as JPEG compression, simulated weather effects (fog, snow), or adjustments to the image's brightness, hue, or contrast, to name a few [Hendrycks and Dietterich, 2018]. The semantic content of the image however, remains unchanged after perceptible or imperceptible perturbations. Hence, we expect the model to output similar predictions for perturbed and unperturbed images.

Applying transformations to the input during training, known as data augmentation, is one of the widely employed techniques for improving robustness. The underlying goal of applying augmentations is to enforce invariance (i.e., consistency) under a predefined set of perturbations. To induce adversarial robustness, worst-case adversarial perturbations are first identified through an optimization procedure and then used to train the model [Madry et al., 2018b, Zhang et al., 2019]. For robustness against perceptible noise, augmentation strategies have evolved from simple transformations such as horizontal flips and rotations to more complex augmentations like MixUp [Zhang et al., 2018], CutMix [Yun et al., 2019], and AugMix [Hendrycks et al., 2020].

There is an observable divide in the treatment of these two types of robustness [Liu et al., 2023a]. Adversarial noises are generated via an optimization process, whereas augmentations are defined heuristically by domain experts. It has also been observed that standard data augmentation strategies, in isolation, do not improve adversarial robustness [Gowal et al., 2021, Rice et al., 2020, Rebuffi et al., 2021]. Additionally, adversarial training (training with adversarial perturbations) often leads to a drop in performance

Submitted to the 40th Conference on Uncertainty in Artificial Intelligence (UAI 2024). **To be used for reviewing only**.

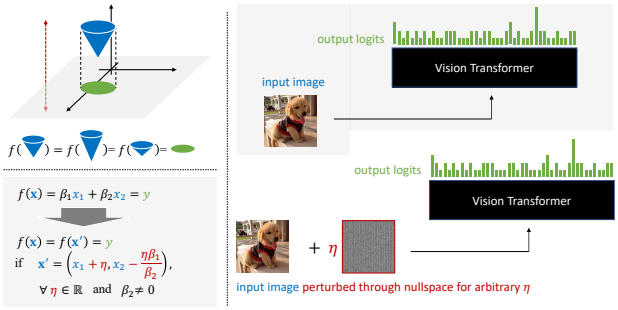

Figure 1: **An illustration of the nullspace in three cases (projection function case, left top; linear function case, left bottom; vision transformer case, right)**. For the functions in these three cases, there exists some nullspace, and the output of the function with respect to the input will remain the same no matter how much perturbation is introduced to the input along the nullspace. Also, the nullspace is function-specific (model-specific) and will not vary for different samples.

on non-adversarial images [Madry et al., 2018b, Zhang et al., 2019, Clarysse et al., 2023].

We consider robustness to be agnostic to the noise type and a property of the model. To this end, we consider the nullspace as the central theme of our study. The nullspace, a fundamental concept in linear algebra, refers to the subspace of a domain that is mapped to zero by a linear mapping. By definition, it is closed under addition and scalar multiplication, implying that any vector from the nullspace, when added to the input of the linear mapping, does not alter its output. In Figure 1, we present the concept of nullspace from different perspectives.

In this paper, firstly, we identify that various off-the-shelf pre-trained ViT models exhibit a non-trivial nullspace due to the presence of a linear patch embedding layer. As the patch embedding layer forms the first block of a ViT, any invariance to the patch embedding block implies invariance to the complete model. Hence, by extension a non-trivial nullspace also exists for ViTs. Furthermore, we analogously define the approximate nullspace of the transformer encoder to dissect its robustness behavior. For non-linear blocks of ViTs, we used an optimization method to synthesize noise vectors which (approximately) exhibit properties of nullspace elements. Lastly, we propose a fine-tuning approach of utilizing these synthesized nullspace-like elements as an additive augmentation to the training data. By encouraging invariance to these elements, we fine-tune the model parameters to enlarge its approximate nullspace, which in-turn boosts the model performance on general robustness.

The main contributions of our paper include:

- We find rich connections between the robustness of vision transformers to the algebraic notion of nullspace, providing fresh insights into the intrinsic properties impacting model robustness. Our claims are substantiated by experimental results showing that enlarging the approximate nullspace effectively improves the model robustness.
- We conduct comprehensive analysis on the existence of nullspace within transformer models. We establish the existence of nullspace at the patch embedding layer, and empirically identify an approximate nullspace at the non-linear encoder level of transformers by validating their algebraic properties.
- We propose an effective data augmentation method exploiting and enlarging the model's approximate nullspace, which enhances model robustness without architectural modifications and only involves fine-tuning with minimal additional data. Our method is empirically validated across multiple benchmark datasets, showing significant robustness improvements against adversarial and out-of-distribution scenarios.

2 RELATED WORK

Data augmentation and Invariance: Data augmentation enforces invariance by training the model to make similar predictions under different views of the input image. In theory, data augmentation can provide a better estimate of the statistical risk [Chen et al., 2020, Shao et al., 2022]. However, applying a wrong augmentation can also lead to a drop in performance [Chen et al., 2020, Lyle et al., 2020, Shao et al., 2022].

For images, augmentations have evolved from simple left-right flipping, cropping and rotation to advanced image composition techniques such as MixUp [Zhang et al., 2018] and CutMix [Yun et al., 2019]. The practice of constructing sequences of augmentations from a set of pre-defined augmentations has gained popularity in recent years. For a specific task, AutoAugment searches for an optimal policy to combine multiple augmentations. TrivialAugment Müller and Hutter [2021] and RandAug Cubuk et al. [2020] improve on the efficiency of chaining augmentations together. AugMix Hendrycks et al. [2020] integrates multiple simple transformations tied together with a consistency loss. Differentiable augmentations computes gradients w.r.t the transformations while optimising for a specific task Li et al. [2020], Chatzipantazis et al. [2023]. Hounie et al. [2023] formulates data augmentation as an invariance-constrained learning problem. They rely on a relaxed notion of invariance to learn distribution over the augmentations. Unlike existing methods, in this work, we do not rely on pre-defined augmentations.

Robustness in ViTs: Emerging research has unveiled the robustness of Vision Transformers (ViTs) over Convolutional Neural Networks (CNNs) [Shao et al., 2021, Paul and Chen, 2022], emphasizing the low transferability of adversarial instances between these architectures [Mahmood

et al., 2021], despite some counter-points [Bai et al., 2021]. ViTs exhibit insensitivity to patch-based transformations that significantly distort original semantics, suggesting their reliance on robust yet non-indicative features [Qin et al., 2022].

Various methods have emerged aiming to enhance the robustness of transformer-based models. Predominantly, these methods are model-agnostic, deploying techniques like data augmentation [Xiao et al., 2023, Esser et al., 2021, Steiner et al., 2022, Liu et al., 2022] and regularization [Chen et al., 2022b, Steiner et al., 2022, Chefer et al., 2022a], aligning with the overarching methodology in robustness studies [Wang et al., 2022b, Liu et al., 2023b]. For instance, Xiao et al. [2023] augments training data by masking image patches based on the class activation map and refilling them with randomly sampled images. Chen et al. [2022b] utilized a sharpness-aware optimizer to encourage a smooth loss landscape of the converged model. Despite the variety, a common theme among these approaches is their emphasis on external modifications or general optimization methods, overlooking the intrinsic properties of the models under consideration.

Nullspace and Neural Networks: To the best of our knowledge, the earliest work investigating neural networks alongside nullspaces corresponds to the study by Goggin et al. [1992]. They studied the universal approximation capabilities of a multi-layered perceptrons by comparing the outputs and nullspace of inputs. Through a classical example of *learning XOR* they showed that with the use of hidden layers, an MLP is able to construct a transformation which maps input to targets even if the target happens to be in the nullspace of the input. In a much recent work, Sonoda et al. [2021] mathematically specified the behavior of nullspace, but only for fully connected networks. On the application side, for a continual learning setting, Wang et al. [2021] proposed to map new tasks to the nullspace of the existing tasks. Lastly as a novel architecture, Abdelpakey and Shehata [2020] proposed NullSpaceNet which maps inputs from the same category to a joint-nullspace instead of a feature space.

3 NULLSPACE AND INVARIANCE

A mapping $f : \mathcal{X} \to \mathcal{Y}$ being invariant to some noise $\mathbf{v}$ implies:

$$f(\mathbf{x} + \mathbf{v}) = f(\mathbf{x}) \quad \forall \mathbf{x} \in \mathcal{X}. \tag{1}$$

Interestingly, invariance under an additive noise has high similarity to the concept of nullspace. Formally, nullspace of a linear mapping f is a set $\mathcal{N} = \{\mathbf{v} \in \mathcal{X} | f(\mathbf{v}) = 0\}$. Appendix A introduces some basic properties of the nullspace. For a non-trivial nullspace, $\mathcal{N} \neq \phi$, $f(\mathbf{x} + \mathbf{v}) = f(\mathbf{x}), \forall \mathbf{v} \in \mathcal{N}, \forall \mathbf{x} \in \mathcal{X}$. This shows that the linear mapping is inherently invariant to the noise vector sampled from its nullspace. For brevity, we refer to this noise vector as **nullspace noise**.

Table 1: **Empirically computed nullspace dimensions for the pre-trained ViT models.** For the cases where the embedding dimension is greater than the input dimension, the nullspace must be trivial, with dimension being 0.

Model	Patch Size	Embedding Dimension	Nullspace Dimension
`ViT-tiny`	16×16	192	576
`ViT-small`	32×32	384	2688
`ViT-small`	16×16	384	384
`ViT-base`	32×32	768	2304
`ViT-base`	16×16	768	2
`ViT-base`	8×8	768	0
`ViT-large`	32×32	1024	2048
`ViT-large`	16×16	1024	0

ViTs, like other deep learning models, are non-linear. Nonetheless, we can still identify a nullspace within its domain, as discussed in Section 3.1.

3.1 NON-TRIVIAL NULLSPACE

Vision transformer as introduced by Dosovitskiy et al. [2021] is a function f_ω with ω as the trainable weights. The function takes as input an image $\mathbf{x} \in \mathcal{X}^{c \times h \times w}$ and outputs a classification response $\mathbf{y} \in \mathcal{Y}^k$ over k categories. c is the number of channels (typically 3 for red, green, and blue), h, w correspond to height and width of the input image. This neural network function can be broken down into 3 stages, namely:

- *patch embedding stage*, $f_\theta : \mathcal{X}^{c \times r \times r} \to \mathcal{U}^d$. This steps projects the input image patch of predetermined dimensions c, r and r to a one-dimensional embedding of length d. It is ensured that patches have no overlaps between them. Hence, the number of such non-overlapping patches generated from the input image are $m = \frac{h \times w}{r^2}$.
- *self-attention stage*, $f_\phi : \mathcal{U}^{(m+1) \times d} \to \mathcal{V}^{(m+1) \times d}$. In the next step, the generated patch embeddings are passed through layers of self-attention modules to process long range interactions amongst them. Apart from the m patch embeddings an additional embedding in form of `cls` token is utilised in this step.
- *classification stage*, $f_\psi : \mathcal{V}^d \to \mathcal{Y}^k$. The final step is to perform the k-way classification. For this, we simply keep the processed encoding corresponding to `cls` token and project it through a linear classification layer.

The nullspace of a vision transformer comes from the fact that its first layer is a linear transformation layer.

As per the rank-nullity theorem, a non-trivial nullspace of the patch embedding layer always exists if $cr^2 > d$. In practice, for many `ViT` based architectures, we find that this is the case. In Table 1, we report the identified nullspace dimensions for off-the-shelf pre-trained ViT models.

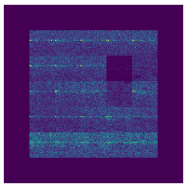

(a) Sample nullspace noise

(b) Clean input image

(c) Noisy input image

Figure 2: **An example of nullspace noise.** We show (a) sample input image, (b) noise generated by the basis vectors of the nullspace and (c) noisy image as a result of adding the nullspace noise to the input. Model's predictions for the clean and noisy inputs are identical.

Given the weights of the patch embedding layer f_θ, finding its nullspace is a standard practice [Kwak and Hong, 2004, Strang, 2009b,a]. Let $B_\theta = \{\mathbf{b}_1, \mathbf{b}_2, \dots \mathbf{b}_k\}$ be the k basis vectors for this nullspace. As per the axioms of nullspace (A), we can sample an element from $\mathcal{N}_\theta$ as:

$$\mathbf{v} = \lambda_1 \mathbf{b}_1 + \lambda_2 \mathbf{b}_2 + \cdots + \lambda_d \mathbf{b}_k. \tag{2}$$

The property of such a sample will be that the output of the patch embedding will effectively remain preserved, $f_\theta(\mathbf{x} + \mathbf{v}) = f_\theta(\mathbf{x})$. Since the output after the first layer remains unaffected, the final output of the classification remains unchanged. In this manner, **nullspace of patch embedding also serves as a subset of the nullspace of the vision transformer**. In Figure 2, we provide visualisation of noise synthesized using basis vectors. This noise can be added to *any* input image with complete invariance.

In Section 3.2, we explore if it possible to learn a nullspace-like counterpart for the non-linear blocks of ViTs.

3.2 THE ENCODER-LEVEL NULLSPACE

So far we have demonstrated that a non-trivial nullspace exists for the patch embedding layer, and hence the entire vision transformer is invariant to all perturbations in that space. We move further down the structure of ViT and investigate whether the encoder is also invariant to certain perturbations. To recall, self-attention stage applies a series of *QKV* attention operations followed by normalization and non-linear transformations. The overall operation is thus non-linear, which means the notion of nullspace cannot be directly applied to f_ϕ.

Regardless, we can still attempt to preserve the axiom of most interest to us, *closeness under vector addition*. This is because we can always formulate data augmentation as a process of adding noise to the input. We attempt the preservation through considering the property of certain noise vectors that, when added to any input, does not disturb the output of a function. Therefore, instead of looking for a vector space, we can instead search for a set with the following property:

$$\tilde{\mathcal{N}}_\phi = \{\mathbf{v} | f(\mathbf{u} + \mathbf{v}) = f(\mathbf{u}) \quad \forall \mathbf{u} \in \mathcal{U}\}, \tag{3}$$

i.e. adding elements from $\tilde{\mathcal{N}}_\phi$ to the input of f_ϕ has no impact on the output. Here, we use the tilde accent $\tilde{\cdot}$ to distinguish $\tilde{\mathcal{N}}_\phi$ from the nullspace $\mathcal{N}_\phi$.

For the patch embedding layer f_θ discussed in Section 3.1 , it is easy to verify that any vector sampled from its nullspace $\mathcal{N}_\theta$ satisfies this property and thus belongs to $\tilde{\mathcal{N}}_\theta$. To study this property in nonlinear functions, we extend the definition of nullspace in linear algebra, and refer to $\tilde{\mathcal{N}}_\phi$ as the *encoder-level nullspace* of transformer. If such a space exists, it directly implies that the transformer model is robust to certain perturbations in the input space. Our theoretical analysis established the following sufficient conditions for the existence of a nontrivial encoder-level nullspace. (The complete proof is given in Appendix A.)

Proposition 1. *Consider a self-attention layer with h heads and $\{(\mathbf{Q}_i, \mathbf{K}_i, \mathbf{V}_i)\}_{i=1}^h$ as its query, key and value projection matrices. If the following conditions are met*

1. *$\mathbf{Q}_i \mathbf{K}_i^\top$ is symmetric for $i = 1, \dots, h$*
2. *The row space $\mathrm{R}(\mathbf{V}_i^\top) \subseteq \mathrm{R}(\mathbf{Q}_i \mathbf{K}_i^\top)$ for $i = 1, \dots, h$*
3. *for some $m \neq n$, $\mathbf{Q}_m \mathbf{K}_m^\top$ has colinearity with $\mathbf{Q}_n \mathbf{K}_n^\top$, i.e. for some k the kth row of $\mathbf{Q}_m \mathbf{K}_m^\top$, denoted as $\mathbf{r}_{m,k}$, satisfies $\mathbf{r}_{m,k} \neq \mathbf{0}$ and $\mathbf{r}_{m,k} \in \mathrm{R}(\mathbf{Q}_n \mathbf{K}_n^\top)$*

then there exists at least one $\mathbf{W}$ such that $\mathbf{W} \neq \mathbf{0}$ and $\mathrm{head}_i(\mathbf{X} + \mathbf{W}) = \mathrm{head}_i(\mathbf{X})$ for all attention head i in this layer and arbitrary $\mathbf{X}$.

Remark 1. Condition 1 can be met if $\mathbf{Q}_i$ and $\mathbf{K}_i$ satisfy some special relation. For example, let $\mathbf{PDP}^{-1}$ be a diagonalization of a real symmetric matrix $\mathbf{A}$. If $\mathbf{Q}_i = \mathbf{BP}$ and $\mathbf{K}_i = \mathbf{B}(\mathbf{P}^{-1})^\top \mathbf{D}$, then we have $\mathbf{Q}_i \mathbf{K}_i^\top = \mathbf{BAB}^\top$ to be symmetric.

In addition, evidence has shown that, $\mathbf{Q}_i \mathbf{K}_i^\top$ can be empirically symmetric, especially for ViTs, when the attention heads are visualized and correlation of parameters is calculated [Yeh et al., 2023].

3.3 SYNTHESIZING (APPROXIMATE) NULLSPACE NOISE

Although our theory suggests a sufficient condition for the existence of encoder-level nullspace, analytically finding $\tilde{\mathcal{N}}_\phi$ or probing its existence for generic transformers is challenging. Thus, as an exploratory experiment, we employ a numeric method: we search for individual element, $\tilde{\mathbf{v}}_\phi$, of this set. This element is an additive perturbation that brings minimal influence to the output of f_ϕ on the data distribution. We introduce a regularization term on the norm of $\tilde{\mathbf{v}}_\phi$

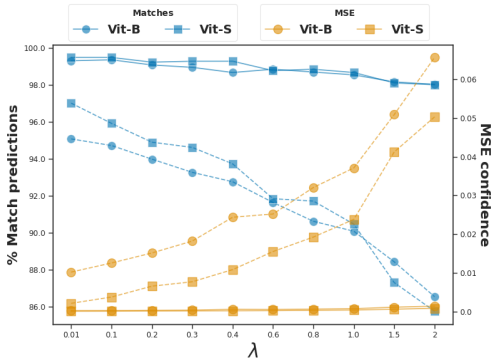

(a) Noise influence on the model output under different regularization strengths

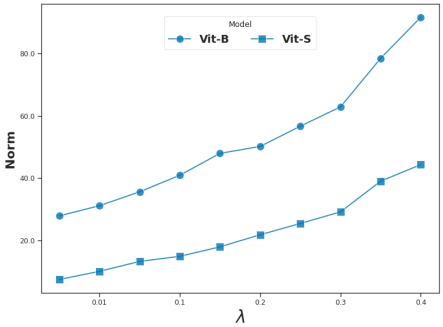

(b) ℓ_2 norm of learned noise under different regularization strengths

Figure 3: **Exploratory experiments on the encoder-level nullspace.** (a) Solid lines (–) represents the model performance under the learned noise, and dashed lines $(\cdots)$ represent the performance after random permutation of the elements of the learned noise vector. (b) by changing the regularization strengths, we explore noise in the encoder-level nullspace at different magnitudes.

to prevent the trivial solution of $\mathbf{0}$.

$$\mathcal{L}_\phi(\tilde{\mathbf{v}}) = \underbrace{\mathbb{E}_{\mathbf{u}\in\mathcal{D}} \left\| f_\psi(f_\phi^0(\mathbf{u}+\tilde{\mathbf{v}})) - f_\psi(f_\phi^0(\mathbf{u}))\right\|}_{\mathfrak{I}} - \lambda \log(\|\tilde{\mathbf{v}}\|). \tag{4}$$

Here, $\|\cdot\|$ is the ℓ_2 norm, f_ϕ^0 is the representation of the `cls` token output by f_ϕ, and λ is the regularization coefficient. $\mathfrak{I}$ resembles a weaker notion of invariance compared to Equation (1). This relaxed definition of invariance has been utilised in previous studies [Wang et al., 2022a, Hounie et al., 2023]. However, unlike prior work, we are directly learning the perturbation and not searching for an optimal transformation from a set of pre-defined transformations. Also, the noise being generated is for the encoder and not at the input level of the model.

We find that simple gradient descent with Equation 4 works well in practice. Note that $\mathcal{L}_\phi(\tilde{\mathbf{v}})$ could potentially be unbounded below as $\|\mathbf{v}\| \to \infty$ due to the second term. Future work may prevent the trivial solution by using a lower bound on the noise norm for constrained optimization.

Equation (4) minimizes the ℓ_2 norm between the predicted logits with and without the noise. Alongside the self-attention stage, we have also incorporated the classification stage into the loss, since the target of our study is to minimize the impact on the final output of the network. To learn the noise vector, we initialize $\tilde{\mathbf{v}}$ by sampling from a uniform distribution, and minimize the loss with gradient descent. We use ViT-S and ViT-B models with patch size 32 for evaluation. We employ ImageNette [Howard, 2018] as the dataset for this experiment, which is a subset of ImageNet consisting of 10 categories. We learn $\tilde{\mathbf{v}}$ on the training dataset (≈ 9500 images) and perform evaluation on the validation set (≈ 4000 images).

To quantitatively evaluate learned $\tilde{\mathbf{v}}_\phi$, in Figure 3 (a) we report the percentage of matching classifications with and without learned nullspace noise, and the mean squared error computed at the output probabilities (hereafter "MSE probability"). We consider a prediction to be matched if the assigned category for input is the same with and without adding the perturbation. By varying the regularization strength, we get noise vectors of different magnitude (Figure 3 (b)), all being fairly benign to the model's predictions. However, if we randomly reset the vectors' direction by permuting their elements, the noise significant degrades the model's predictions.

The experiment shows the feasibility of learning elements that approximately conform to our definition of encoder-level nullspace with good precision, and also indicates that at different magnitudes there are certain directions in the input space toward which the perturbation is fairly benign to the model.

4 NULLSPACE NOISE AUGMENTED FINETUNING

In this section, we investigate the application of the synthesized nullspace noise. As we discussed previously, the model is weakly invariant to the learnt noise ($\mathfrak{I}$ in Equation (4)) and the set as a result of this relaxed notion is an approximate nullspace. To more accurately quantify this, we define ϵ-approximate nullspace as follows:

$$\tilde{\mathcal{N}}_\phi(\epsilon) = \{\tilde{\mathbf{v}} | \mathbb{E}_{\mathbf{u}\in\mathcal{D}} \left\| f(\mathbf{u}+\tilde{\mathbf{v}}) - f(\mathbf{u})\right\| \leq \epsilon\}. \tag{5}$$

where $f(\cdot) = \text{Softmax}(f_\psi(f_\phi^0(\cdot)))$.It is easy to verify that $\forall \epsilon > 0, \mathbf{0} \in \tilde{\mathcal{N}}_\phi(\epsilon)$, and that $\forall \epsilon_2 > \epsilon_1 > 0, \tilde{\mathcal{N}}_\phi(\epsilon_1) \subseteq \tilde{\mathcal{N}}_\phi(\epsilon_2)$.

We believe that the existence of approximate noise vectors is a model property. As these vectors exhibit relaxed invariance, we also believe that they play a key role in model's inherent robustness under a variety of distribution shifts. Hence, if we can further improve invariance on approximate

nullspace elements, we can potentially make the model more robust. With this belief, **we propose to fine-tune a pre-trained ViT with the learnt nullspace noise vector as an added (encoder level) input perturbation.** The motivation behind this is to enlarge the (approximate nullspace) set of noise vectors to which the model is invariant.

Formally, we employ a bi-level optimization approach, where the inner problem finds the best noise vector and the outer problem finds the model that is the most tolerant to such noise, as shown below.

$$\begin{aligned} \min_{\phi} \quad & \mathbb{E}_{\mathbf{u}\in\mathcal{D}}\, \ell(f_\psi(f_\phi^0(\mathbf{u}+\tilde{\mathbf{v}}_\phi^*)), \mathbf{y}) \\ \text{where} \quad & \tilde{\mathbf{v}}_\phi^* = \arg\max_{\tilde{\mathbf{v}}} \|\tilde{\mathbf{v}}\| \quad \text{s.t.} \;\; \tilde{\mathbf{v}} \in \mathcal{N}_\phi(\epsilon). \end{aligned} \tag{6}$$

Here, $\ell(\cdot)$ is the cross-entropy loss. While this optimization problem can also be solved in different ways, we use an efficient heuristic: we initialize the noise with a large enough sampling limit, minimize $\mathcal{L}_\phi(\tilde{\mathbf{v}})$ by gradient descent according to the loss function in Equation 7, and early stop it as soon as it enters $\tilde{\mathcal{N}}_\phi(\epsilon)$, as shown in Equation 8.

$$\mathcal{L}_\phi(\tilde{\mathbf{v}}) = \mathbb{E}_{\mathbf{u}\in\mathcal{D}}\, \|f_\psi(f_\phi^0(\mathbf{u}+\tilde{\mathbf{v}})) - f_\psi^0(f_\phi(\mathbf{u}))\| \tag{7}$$

$$\hat{\mathbf{v}}^* = \mathrm{SGD}(\mathcal{L}_\phi(\tilde{\mathbf{v}}), \tilde{\mathbf{v}}_0, \epsilon). \tag{8}$$

Here, $\hat{\mathbf{v}}_\phi^*$ is the approximate solution for $\tilde{\mathbf{v}}_\phi^*$, $\mathrm{SGD}(\mathcal{L}_\phi(\tilde{\mathbf{v}}), \tilde{\mathbf{v}}_0, \epsilon)$ denotes the gradient descent algorithm that minimizes the loss $\mathcal{L}_\phi(\tilde{\mathbf{v}})$ starting from its initial value $\tilde{\mathbf{v}}_0$ until it satisfies the condition $\mathcal{L}_\phi(\tilde{\mathbf{v}}) < \epsilon$. The noise norm starts from a large value and gets gradually reduced during the process. When early stopping is triggered, we obtain noise vectors that are close to the boundary of the ϵ-approximate nullspace. For more details of our method, please refer to Algorithm 1 in Appendix C.

5 EXPERIMENTS

5.1 IMPLEMENTATION DETAILS

In this section, we conducted comprehensive evaluation of our nullspace augmentation method (Section 4) on several benchmarks. By making the model more tolerant to noise in the ϵ-approximate nullspace, we hope to expand the nullspace itself and observe its effect on the model's robustness under different settings.

Starting from a pretrained model, we use the ϵ-approximate nullspace noise as data augmentation to fine-tune the model. The noise is generated every 40 training steps according to Equation (8) with an ϵ of 0.03. The experiment was done within one epoch of training on the ImageNet-1k [Deng et al., 2009] dataset. We used the vanilla `ViT-small` and `ViT-base` models, and `ViT-base(DAT)` which is the current SOTA on ImageNet-C dataset on the EasyRobust benchmark[1], trained using Discrete Adversarial Training [Mao et al., 2022a]. We evaluated the model performance in a wide range of settings to test its performance on the i.i.d dataset, under adversarial attacks and distribution shifts. For adversarial attacks we utilize FGSM [Goodfellow et al., 2015], DamageNet [Chen et al., 2022a], PatchFool [Fu et al., 2022] and CW [Carlini and Wagner, 2017]. Among them, FGSM and CW are gradient-based white-box attacks, DamageNet consists of pre-generated adversarial examples, and PatchFool targets localized, adversarial patches of an image. We consider the out-of-distribution (OOD) evaluation setting wherein categories in the test and training set are consistent, the key distinction lies in the nature of the images present during the test. OOD benchmarks utilized in our study consist of unseen variations of the training categories. We employ the datasets of ImageNet-C [Hendrycks and Dietterich, 2018], ImageNet-A [Hendrycks et al., 2021b], ImageNet-V2 [Recht et al., 2019], Imagenet-R [Hendrycks et al., 2021a], ImageNet-Sketch [Wang et al., 2019] and Stylized-Imagenet [Geirhos et al., 2018]. ImageNet-C consists of validation images modified by applying corruptions in the form of weather effects, noises, etc. ImageNet-A applies the imagenet objects in hard contexts. ImageNet-R and ImageNet-Sketch consist of imagenet categories in different art forms. ImageNet-Stylized applies texture transfer onto the ImageNet validation images to create shape-texture contradictions.

We use the EasyRobust library [Mao et al., 2022b] for code implementation and the checkpoints of `ViT-base(DAT)`. For more implementation details please see our supplementary document.

5.2 EXPERIMENT: ROBUSTNESS EVALUATION

We evaluate the effect of nullspace training for improving the robustness of vision transformers under different settings. We use the official mCE score as the evaluation metric for ImageNet-C, where lower mCE indicates better robustness, and used the accuracy score for all the other settings. We used $100 - \text{mCE}$ before taking the average over all settings.

The result in Table 2 shows that our nullspace augmentation method consistently improves the robustness of models under distribution shifts and adversarial attacks, yielding a large gain in average performance for the vanilla `ViT-small` and `ViT-base model`, and slightly outperforms various baselines consistently while also slightly outperforming DAT. This not only shows that our nullspace training method is effective but also validates our previous hypothesis about the connection between the tolerance to nullspace and the robustness of transformer models.

5.3 EXPERIMENT: ADVERSARIAL FINETUNING

In this experiment, we compare our method with fine-tuning using two PGD adversarial training methods, Madry [Madry

[1] https://github.com/alibaba/easyrobust

Table 2: **Effect of nullspace training on different models evaluated on multiple benchmark datasets.** Excluding DAT, vanilla ViT-S and ViT-B, the values for the baselines are directly reported from the corresponding papers. For DAT, we report the reproduced results following their evaluation setting.

Methods	Clean	Adversarial Robustness				Out of Distribution Robustness						Average
		PatchFool	CW	FGSM	DamageNet	A	C↓	V2	R	Sketch	Stylized	
ViT-S	74.19	0.68	4.63	13.79	29.82	16.35	71.13	62.51	34.67	14.26	12.15	26.54
ViT-S + NS (ours)	**77.47**	**19.10**	**9.37**	**25.95**	**32.43**	**20.77**	**55.98**	**66.5**	**41.61**	**25.67**	**16.02**	**34.45**
ViT-B	77.68	15.92	12.54	25.65	38.69	23.88	62.16	66.05	41.63	16.31	17.97	34.01
ViT-B + MixUp [Zhang et al., 2018]	77.80	–	–	–	–	12.20	61.80	–	34.90	–	–	–
ViT-B + RandAugment [Cubuk et al., 2020]	79.10	–	–	–	–	–	43.60	–	23.00	–	–	–
ViT-B + PR [Qin et al., 2022]	78.20	–	–	–	–	–	47.60	–	21.40	–	–	–
ViT-B + RandAugment + PR	79.30	–	–	–	–	–	43.60	–	23.80	–	–	–
ViT-B + AugMix [Hendrycks et al., 2020]	78.80	–	–	–	–	–	42.20	–	24.90	–	–	–
ViT-B + AugMix + PR	79.30	–	–	–	–	–	**41.60**	–	25.70	–	–	–
ViT-B + SAM [Chen et al., 2022b]	79.90	–	–	–	–	–	43.50	67.50	26.40	–	–	–
RobustViT-B [Chefer et al., 2022b]	80.40	–	–	–	–	23.00	–	69.80	35.40	**35.80**	–	–
ViT-B + NS (ours)	**81.42**	**23.52**	**14.23**	**36.50**	**40.44**	**24.55**	47.82	**70.25**	**44.85**	26.35	**19.02**	**39.39**
ViT-B + DAT[Mao et al., 2022a]	**81.47**	22.64	23.59	48.80	43.31	23.83	45.95	**70.24**	**48.68**	36.94	**23.99**	43.41
ViT-B + DAT + NS (ours)	81.33	**24.14**	**23.61**	**48.98**	**43.67**	**24.22**	**45.91**	70.14	48.48	**37.25**	23.87	**43.61**

Table 3: **Comparison of nullspace augmented fine-tuning with PGD based adversarial robustness methods of Madry and TRADES.** We report the performance for a ViT-S model.

Method	clean	FGSM	DamageNet	A	C (↓)	V2	R	Sketch	Stylized
ViT-S	74.19	13.79	29.82	16.35	71.13	62.51	34.67	14.26	12.15
Madry	70.53	**39.37**	**49.91**	9.37	81.74	58.88	39.04	21.36	10.76
TRADES	74.02	38.85	36.28	16.53	73.11	63.37	40.86	**26.43**	13.22
Ours	**77.47**	25.95	32.43	**20.77**	**55.98**	**66.5**	**41.61**	25.67	**16.02**

et al., 2018a] and TRADES [Zhang et al., 2019] on the ViT-S model. TRADES, in each training iteration, generates adversarial examples using PGD and updates the model's parameters to minimize the worst-case loss on these adversarial examples while also minimizing the standard classification loss on clean data. Madry, on the other hand, focuses exclusively on minimizing the worst-case loss on adversarial examples.

In Table 3, we observe that Madry and TRADES provide better performance for adversarial evaluation. This is expected as the methods are catered for improving adversarial robustness. However, this exclusivity leads to relatively poorer performance in a wider benchmark evaluation. Compared to our method, Madry and TRADES perform considerably lower in the natural OOD setting.

5.4 ENLARGED APPROXIMATE NULLSPACE

To gain more insight about the dynamics of our nullspace augmentation method, we monitor the l_2 norm of the learned noise and various performance metrics during the training, as shown in Fig. 4. Before the nullspace training, it was hard to optimize the noise into the ϵ region even with increased training, so the norm started with a high value. As the training starts, we find from the experiment log that the noise was

Figure 4: **Change trend of multiple metrics with training steps.** "Adversarial" is the average performance on "FGSM" and "DamageNet" settings, "OOD" is the average score of the six OOD datasets, and "avg" is the total average. All values are divided by their initial values to show the trend more clearly.

always able to enter the ϵ region. In Appendix D, we show the MSE probability of the learned noise vectors, which are smaller than ϵ at each round of noise learning. Also, the norm of the learned noise gradually increases along the process of model fine-tuning. The fluctuation may have mainly resulted from the randomness in mini-batches and the optimization dynamics. The model allows for noises with larger and larger norms to be within ϵ-approximate, which informally suggests an enlarging ϵ-approximate nullspace. Accompanied by the trend is the increase in robustness scores in both OOD and adversarial settings, which corroborates our findings.

5.5 ABLATION STUDY

We conduct an extensive study to analyse the performance of our method under choice of ϵ. Furthermore, we also

Table 4: **Impact of ϵ on the final performance**. Moreover, we also compare our approach against random ϵ noise based finetuning.

ϵ	Finetuning	FGSM	DamageNet	A	C (↓)	V2	R	Sketch	Stylized
0.01	nullspace	26.04	33.65	20.45	56.26	66.47	41.4	23.34	15.85
	random	21.54	28.81	17.07	55.13	61.98	34.97	14.43	12.14
0.03	nullspace	25.95	32.43	20.77	55.98	66.5	41.61	25.67	16.02
	random	23.18	29.61	16.91	54.68	62.2	35.05	14.77	12.34
0.1	nullspace	25.38	33.09	20.16	56.41	66.47	40.42	22.66	15.78
	random	23.93	30.56	16.47	54.52	62.48	34.66	14.99	12.35

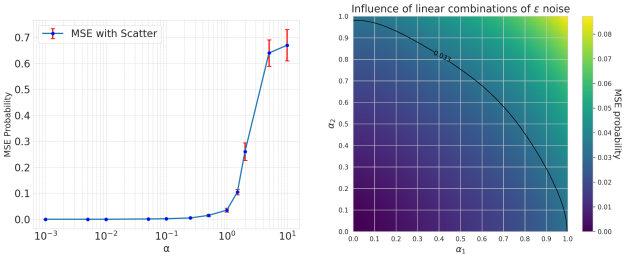

(a) Influence of ϵ noise under multiplication with different α

(b) Influence of ϵ noise under convex combination with different α_1, α_2

Figure 5: Validation of the properties of the ϵ-approximate nullspace.

compare our approach with a simple baseline of using an ϵ noise sampled from a Gaussian distribution.

From Table 4, we can infer that the nullspace noise based finetuning is relatively robust to the choice of ϵ. Moreover, compared to using randomly generated ϵ-noise, our nullspace based training provides significant performance boost. This observation stands across different values of ϵ.

5.6 PROPERTIES OF THE APPROXIMATE NULLSPACE

To explore the property of the ϵ-approximate nullspace, we conduct an experiment to observe the behavior of the learned noise vectors under scalar multiplication and convex combination. For this, we first construct a set of m ϵ-approximate nullspace vectors $\mathbf{V} = \{\mathbf{v}_i\}_{i=1}^{m}$ starting from different random initializations using $\epsilon = 0.033$. For scalar multiplication, we vary the scaling factor α and report the mean influence of $\alpha\mathbf{v}$ on the model's predictions in terms of MSE probabilities (Figure 5(a)). For convex combination, we sample n different pairs of nullspace vectors from $\mathbf{V}$, denoted as $\mathbf{P} = \{(\mathbf{v}_{\mathcal{J}_{k,1}}, \mathbf{v}_{\mathcal{J}_{k,2}})\}_{k=1}^{n}$, where $\mathcal{J}_{k,1}, \mathcal{J}_{k,2} \in \{1, 2, \ldots, m\}, \forall k \in \{1, \ldots n\}$. Then, we vary α_1 and α_2 between $[0, 1]$ with a grid size of 0.1, and for each combination of (α_1, α_2), we evaluate the influence of the convex combination $\alpha_1\mathbf{v}_{\mathcal{J}_{k,1}} + \alpha_2\mathbf{v}_{\mathcal{J}_{k,2}}$ on the model's prediction in MSE probability, averaged over all values of k. In practice we set $m = 100, n = 10$. The influence of the linear combined noise at each point of the grid is visualized as a heatmap as shown in Figure 5(b).

The results in Figure 5 show that the approximate nullspace has similar property to vector space in terms of closure under addition and scalar multiplication within a certain range of coefficients. When the scaling factor $\alpha < 1$, we see a clear trend that the MSE probability of the scaled noise is less than $\alpha\epsilon$. In the linear combination case, the line $\alpha_1 + \alpha_2 = 1$ is well within the contour line of MSE probability being 0.033, showing that the convex combination of a pair of ϵ noise vector is still ϵ-approximate.

6 DISCUSSION

Applications in Model Patenting In addition to the applications we discussed, we consider another potential usage of our findings is to patent a ViT after a model is trained, as the nullspace will be unique property of any set of weights of certain ViT architectures. Different from the existing line of research in model watermarking [Adi et al., 2018, Darvish Rouhani et al., 2019, Le Merrer et al., 2020], the patenting through nullspace will not require any additional steps during training, although will face limited usage scenarios in comparison.

Applications in Image Watermarking Using the nullspace noise, it is possible to apply signatures onto input images without harming the output or operability of the networks. In the supplementary document, we present the cases where certain marks in form of nullspace noise can be superimposed on any desired input image.

Potential Limitation about the Nullspace Approximation Different from the nullspace defined in linear algebra, the nullspace of the entire ViT can only be approximated because of the non-linearity in the network architecture. However, it is worthy mentioning that we can still calculate the exact nullspace of ViT if we only consider the patch embedding layer, through which, our results will qualitatively deliver the same message, but with quantitative differences.

7 CONCLUSION

In this work, we have explored the concept of nullspace in Vision Transformers (ViTs) to understand their robustness.

Our findings demonstrate that a non-trivial nullspace indeed exists for Vision Transformers, a direct consequence of the patch embedding layer. This discovery implies that there are elements that, when added to an input, do not affect the output of the network, potentially offering an explanation for the robustness exhibited by ViTs. Moreover, we have extended the definition of nullspace, preserving a property that implies invariance of a mapping's output to input perturbations, and empirically identified a space that exhibits such property within the input space of the non-linear transformer encoder.

By linking the presence of nullspace with our extended definition to the general robustness of a network, we were able to devise a new approach to improve the robustness of ViTs. Our empirical results suggest that fine-tuning ViTs with the learnt nullspace noise can significantly enhance their robustness to a variety of robustness benchmarks. This method offers a new direction for data augmentation and model training, which could be beneficial for further research.

References

Mohamed H. Abdelpakey and Mohamed S. Shehata. Nullspacenet: Nullspace convoluional neural network with differentiable loss function. *CoRR*, abs/2004.12058, 2020. URL https://arxiv.org/abs/2004.12058.

Samira Abnar and Willem Zuidema. Quantifying attention flow in transformers. In *Proceedings of the 58th Annual Meeting of the Association for Computational Linguistics*, pages 4190–4197, Online, July 2020. Association for Computational Linguistics. doi: 10.18653/v1/2020.acl-main.385. URL https://aclanthology.org/2020.acl-main.385.

Yossi Adi, Carsten Baum, Moustapha Cisse, Benny Pinkas, and Joseph Keshet. Turning your weakness into a strength: Watermarking deep neural networks by backdooring. In *27th USENIX Security Symposium (USENIX Security 18)*, pages 1615–1631, 2018.

Ali Al-Haj. Combined dwt-dct digital image watermarking. *Journal of computer science*, 3(9):740–746, 2007.

Alaaeldin Ali, Hugo Touvron, Mathilde Caron, Piotr Bojanowski, Matthijs Douze, Armand Joulin, Ivan Laptev, Natalia Neverova, Gabriel Synnaeve, Jakob Verbeek, et al. Xcit: Cross-covariance image transformers. *Advances in neural information processing systems*, 34:20014–20027, 2021.

Yutong Bai, Jieru Mei, Alan L Yuille, and Cihang Xie. Are transformers more robust than cnns? In M. Ranzato, A. Beygelzimer, Y. Dauphin, P.S. Liang, and J. Wortman Vaughan, editors, *Advances in Neural Information Processing Systems*, volume 34, pages 26831–26843. Curran Associates, Inc., 2021. URL https://proceedings.neurips.cc/paper/2021/file/e19347e1c3ca0c0b97de5fb3b690855a-Paper.pdf.

Hal Berghel. Digital watermarking makes its mark. *Networker*, 2(4):30–39, 1998.

Vivekananda Bhat, Indranil Sengupta, and Abhijit Das. An adaptive audio watermarking based on the singular value decomposition in the wavelet domain. *Digital Signal Processing*, 20(6):1547–1558, 2010.

N. Carlini and D. Wagner. Towards evaluating the robustness of neural networks. In *2017 IEEE Symposium on Security and Privacy (SP)*, pages 39–57, Los Alamitos, CA, USA, may 2017. IEEE Computer Society. doi: 10.1109/SP.2017.49. URL https://doi.ieeecomputersociety.org/10.1109/SP.2017.49.

Evangelos Chatzipantazis, Stefanos Pertigkiozoglou, Kostas Daniilidis, and Edgar Dobriban. Learning augmentation distributions using transformed risk minimization. *Transactions on Machine Learning Research*, 2023. ISSN 2835-8856. URL https://openreview.net/forum?id=LRYtNj8Xw0.

Hila Chefer, Shir Gur, and Lior Wolf. Transformer interpretability beyond attention visualization. In *Proceedings of the IEEE/CVF Conference on Computer Vision and Pattern Recognition (CVPR)*, pages 782–791, June 2021.

Hila Chefer, Idan Schwartz, and Lior Wolf. Optimizing relevance maps of vision transformers improves robustness. In Alice H. Oh, Alekh Agarwal, Danielle Belgrave, and Kyunghyun Cho, editors, *Advances in Neural Information Processing Systems*, 2022a. URL https://openreview.net/forum?id=upuYKQiyxa_.

Hila Chefer, Idan Schwartz, and Lior Wolf. Optimizing relevance maps of vision transformers improves robustness. In S. Koyejo, S. Mohamed, A. Agarwal, D. Belgrave, K. Cho, and A. Oh, editors, *NeurIPS*, volume 35, pages 33618–33632. Curran Associates, Inc., 2022b. URL https://proceedings.neurips.cc/paper_files/paper/2022/file/d9fa720cf96f7c18ac4d9e04270f0bbf-Paper-Conferer
pdf.

Shuxiao Chen, Edgar Dobriban, and Jane H Lee. A group-theoretic framework for data augmentation. *The Journal of Machine Learning Research*, 21(1):9885–9955, 2020.

Sizhe Chen, Zhengbao He, Chengjin Sun, Jie Yang, and Xiaolin Huang. Universal adversarial attack on attention and the resulting dataset damagenet. *IEEE Transactions on Pattern Analysis and Machine Intelligence*, 44(4):2188–2197, 2022a. doi: 10.1109/TPAMI.2020.3033291.

Xiangning Chen, Cho-Jui Hsieh, and Boqing Gong. When vision transformers outperform resnets without pretraining or strong data augmentations. In *ICLR*, 2022b. URL https://openreview.net/forum?id=LtKcMgGOeLt.

Jacob Clarysse, Julia Hörrmann, and Fanny Yang. Why adversarial training can hurt robust accuracy. In *ICLR*, 2023. URL https://openreview.net/forum?id=-CA8yFkPc7O.

Ekin Dogus Cubuk, Barret Zoph, Jon Shlens, and Quoc Le. Randaugment: Practical automated data augmentation with a reduced search space. In H. Larochelle, M. Ranzato, R. Hadsell, M.F. Balcan, and H. Lin, editors, *NeurIPS*, volume 33, pages 18613–18624. Curran Associates, Inc., 2020. URL https://proceedings.neurips.cc/paper_files/paper/2020/file/d85b63ef0ccb114d0a3bb7b7d808028f-Paper.pdf.

Bita Darvish Rouhani, Huili Chen, and Farinaz Koushanfar. Deepsigns: An end-to-end watermarking framework for ownership protection of deep neural networks. In *Proceedings of the Twenty-Fourth International Conference on Architectural Support for Programming Languages and Operating Systems*, pages 485–497, 2019.

Jia Deng, Wei Dong, Richard Socher, Li-Jia Li, Kai Li, and Li Fei-Fei. Imagenet: A large-scale hierarchical image database. In *2009 IEEE conference on computer vision and pattern recognition*, pages 248–255. Ieee, 2009.

Ann-Kathrin Dombrowski, Maximillian Alber, Christopher Anders, Marcel Ackermann, Klaus-Robert Müller, and Pan Kessel. Explanations can be manipulated and geometry is to blame. *Advances in Neural Information Processing Systems*, 32, 2019.

Alexey Dosovitskiy, Lucas Beyer, Alexander Kolesnikov, Dirk Weissenborn, Xiaohua Zhai, Thomas Unterthiner, Mostafa Dehghani, Matthias Minderer, Georg Heigold, Sylvain Gelly, Jakob Uszkoreit, and Neil Houlsby. An image is worth 16x16 words: Transformers for image recognition at scale. *ICLR*, 2021.

Patrick Esser, Robin Rombach, and Bjorn Ommer. Taming transformers for high-resolution image synthesis. In *Proceedings of the IEEE/CVF conference on computer vision and pattern recognition*, pages 12873–12883, 2021.

Yonggan Fu, Shunyao Zhang, Shang Wu, Cheng Wan, and Yingyan Lin. Patch-fool: Are vision transformers always robust against adversarial perturbations? In *International Conference on Learning Representations*, 2022. URL https://openreview.net/forum?id=28ib9tf6zhr.

Robert Geirhos, Patricia Rubisch, Claudio Michaelis, Matthias Bethge, Felix A Wichmann, and Wieland Brendel. Imagenet-trained cnns are biased towards texture; increasing shape bias improves accuracy and robustness. In *International Conference on Learning Representations*, 2018.

Amirata Ghorbani, Abubakar Abid, and James Zou. Interpretation of neural networks is fragile. In *Proceedings of the AAAI conference on artificial intelligence*, volume 33, pages 3681–3688, 2019.

Shelly D. D. Goggin, Karl E. Gustafson, and Kristina M. Johnson. Accessing the null space with nonlinear multilayer neural networks. In Dennis W. Ruck, editor, *Science of Artificial Neural Networks*, volume 1710, pages 308 – 316. International Society for Optics and Photonics, SPIE, 1992. doi: 10.1117/12.140097. URL https://doi.org/10.1117/12.140097.

Ian J. Goodfellow, Jonathon Shlens, and Christian Szegedy. Explaining and harnessing adversarial examples. In Yoshua Bengio and Yann LeCun, editors, *3rd International Conference on Learning Representations, ICLR 2015, San Diego, CA, USA, May 7-9, 2015, Conference Track Proceedings*, 2015. URL http://arxiv.org/abs/1412.6572.

Sven Gowal, Chongli Qin, Jonathan Uesato, Timothy Mann, and Pushmeet Kohli. Uncovering the limits of adversarial training against norm-bounded adversarial examples, 2021.

Dan Hendrycks and Thomas Dietterich. Benchmarking neural network robustness to common corruptions and perturbations. In *International Conference on Learning Representations*, 2018.

Dan Hendrycks, Norman Mu, Ekin Dogus Cubuk, Barret Zoph, Justin Gilmer, and Balaji Lakshminarayanan. Augmix: A simple method to improve robustness and uncertainty under data shift. In *ICLR*, 2020. URL https://openreview.net/forum?id=S1gmrxHFvB.

Dan Hendrycks, Steven Basart, Norman Mu, Saurav Kadavath, Frank Wang, Evan Dorundo, Rahul Desai, Tyler Zhu, Samyak Parajuli, Mike Guo, Dawn Song, Jacob Steinhardt, and Justin Gilmer. The many faces of robustness: A critical analysis of out-of-distribution generalization. In *Proceedings of the IEEE/CVF International Conference on Computer Vision (ICCV)*, pages 8340–8349, October 2021a.

Dan Hendrycks, Kevin Zhao, Steven Basart, Jacob Steinhardt, and Dawn Song. Natural adversarial examples. In *Proceedings of the IEEE/CVF Conference on Computer Vision and Pattern Recognition*, pages 15262–15271, 2021b.

Juyeon Heo, Sunghwan Joo, and Taesup Moon. Fooling neural network interpretations via adversarial model manipulation. *Advances in Neural Information Processing Systems*, 32, 2019.

Ignacio Hounie, Luiz F. O. Chamon, and Alejandro Ribeiro. Automatic data augmentation via invariance-constrained learning. In Andreas Krause, Emma Brunskill, Kyunghyun Cho, Barbara Engelhardt, Sivan Sabato, and Jonathan Scarlett, editors, *ICML*, volume 202 of *Proceedings of Machine Learning Research*, pages 13410–13433. PMLR, 23–29 Jul

2023. URL https://proceedings.mlr.press/v202/hounie23a.html.

Jeremy Howard. Imagenette, 2018. URL https://github.com/fastai/imagenette/.

Alexander Kirillov, Eric Mintun, Nikhila Ravi, Hanzi Mao, Chloe Rolland, Laura Gustafson, Tete Xiao, Spencer Whitehead, Alexander C Berg, Wan-Yen Lo, et al. Segment anything. *arXiv preprint arXiv:2304.02643*, 2023.

Jin Ho Kwak and Sungpyo Hong. *Linear Algebra*. Birkhäuser, Boston, MA, 2004. doi: 10.1007/978-0-8176-8194-4.

Erwan Le Merrer, Patrick Perez, and Gilles Trédan. Adversarial frontier stitching for remote neural network watermarking. *Neural Computing and Applications*, 32(13): 9233–9244, 2020.

Yehao Li, Ting Yao, Yingwei Pan, and Tao Mei. Contextual transformer networks for visual recognition. *IEEE Transactions on Pattern Analysis and Machine Intelligence*, 2022.

Yonggang Li, Guosheng Hu, Yongtao Wang, Timothy M. Hospedales, Neil Martin Robertson, and Yongxin Yang. DADA: differentiable automatic data augmentation. 2020.

Haoyang Liu, Maheep Chaudhary, and Haohan Wang. Towards trustworthy and aligned machine learning: A data-centric survey with causality perspectives. *arXiv preprint arXiv:2307.16851*, 2023a.

Haoyang Liu, Maheep Chaudhary, and Haohan Wang. Towards trustworthy and aligned machine learning: A data-centric survey with causality perspectives, 2023b.

Jihao Liu, Boxiao Liu, Hang Zhou, Hongsheng Li, and Yu Liu. Tokenmix: Rethinking image mixing for data augmentation in vision transformers. In *European Conference on Computer Vision*, pages 455–471. Springer, 2022.

Ze Liu, Yutong Lin, Yue Cao, Han Hu, Yixuan Wei, Zheng Zhang, Stephen Lin, and Baining Guo. Swin transformer: Hierarchical vision transformer using shifted windows. In *Proceedings of the IEEE/CVF International Conference on Computer Vision (ICCV)*, 2021.

Ilya Loshchilov and Frank Hutter. Decoupled weight decay regularization. In *International Conference on Learning Representations*, 2019. URL https://openreview.net/forum?id=Bkg6RiCqY7.

Clare Lyle, Mark van der Wilk, Marta Kwiatkowska, Yarin Gal, and Benjamin Bloem-Reddy. On the benefits of invariance in neural networks. *arXiv preprint arXiv:2005.00178*, 2020.

Aleksander Madry, Aleksandar Makelov, Ludwig Schmidt, Dimitris Tsipras, and Adrian Vladu. Towards deep learning models resistant to adversarial attacks. In *ICLR*. OpenReview.net, 2018a. URL https://openreview.net/forum?id=rJzIBfZAb.

Aleksander Madry, Aleksandar Makelov, Ludwig Schmidt, Dimitris Tsipras, and Adrian Vladu. Towards deep learning models resistant to adversarial attacks. In *International Conference on Learning Representations*, 2018b. URL https://openreview.net/forum?id=rJzIBfZAb.

Kaleel Mahmood, Rigel Mahmood, and Marten Van Dijk. On the robustness of vision transformers to adversarial examples. In *Proceedings of the IEEE/CVF International Conference on Computer Vision*, pages 7838–7847, 2021.

Xiaofeng Mao, YueFeng Chen, Ranjie Duan, Yao Zhu, Gege Qi, Shaokai Ye, Xiaodan Li, Rong Zhang, and Hui Xue'. Enhance the visual representation via discrete adversarial training. In Alice H. Oh, Alekh Agarwal, Danielle Belgrave, and Kyunghyun Cho, editors, *Advances in Neural Information Processing Systems*, 2022a. URL https://openreview.net/forum?id=qtZac7A3-F.

Xiaofeng Mao, Yuefeng Chen, Xiaodan Li, Gege Qi, Ranjie Duan, Rong Zhang, and Hui Xue. Easyrobust: A comprehensive and easy-to-use toolkit for robust computer vision. https://github.com/alibaba/easyrobust, 2022b.

Seyed-Mohsen Moosavi-Dezfooli, Alhussein Fawzi, and Pascal Frossard. Deepfool: A simple and accurate method to fool deep neural networks. In *2016 IEEE Conference on Computer Vision and Pattern Recognition (CVPR)*, pages 2574–2582, 2016. doi: 10.1109/CVPR.2016.282.

Samuel G. Müller and Frank Hutter. Trivialaugment: Tuning-free yet state-of-the-art data augmentation. In *ICCV*, pages 774–782, October 2021.

Anh Nguyen, Jason Yosinski, and Jeff Clune. Deep neural networks are easily fooled: High confidence predictions for unrecognizable images. In *2015 IEEE Conference on Computer Vision and Pattern Recognition (CVPR)*, pages 427–436, 2015. doi: 10.1109/CVPR.2015.7298640.

Sayak Paul and Pin-Yu Chen. Vision transformers are robust learners. *Proceedings of the AAAI Conference on Artificial Intelligence*, 2022.

Vidyasagar M Potdar, Song Han, and Elizabeth Chang. A survey of digital image watermarking techniques. In *INDIN'05. 2005 3rd IEEE International Conference on Industrial Informatics, 2005.*, pages 709–716. IEEE, 2005.

Yao Qin, Chiyuan Zhang, Ting Chen, Balaji Lakshminarayanan, Alex Beutel, and Xuezhi Wang. Understanding and improving robustness of vision transformers

through patch-based negative augmentation. In S. Koyejo, S. Mohamed, A. Agarwal, D. Belgrave, K. Cho, and A. Oh, editors, *NeurIPS*, pages 16276–16289, 2022.

Sylvestre-Alvise Rebuffi, Sven Gowal, Dan Andrei Calian, Florian Stimberg, Olivia Wiles, and Timothy A Mann. Data augmentation can improve robustness. In M. Ranzato, A. Beygelzimer, Y. Dauphin, P.S. Liang, and J. Wortman Vaughan, editors, *NeurIPS*, volume 34, pages 29935–29948. Curran Associates, Inc., 2021. URL https://proceedings.neurips.cc/paper_files/paper/2021/file/fb4c48608ce8825b558ccf07169a3421-Paper.pdf.

Benjamin Recht, Rebecca Roelofs, Ludwig Schmidt, and Vaishaal Shankar. Do imagenet classifiers generalize to imagenet? In *International Conference on Machine Learning*, pages 5389–5400. PMLR, 2019.

Leslie Rice, Eric Wong, and Zico Kolter. Overfitting in adversarially robust deep learning. In Hal Daumé III and Aarti Singh, editors, *Proceedings of the 37th International Conference on Machine Learning*, volume 119 of *Proceedings of Machine Learning Research*, pages 8093–8104. PMLR, 13–18 Jul 2020. URL https://proceedings.mlr.press/v119/rice20a.html.

Ramprasaath R. Selvaraju, Michael Cogswell, Abhishek Das, Ramakrishna Vedantam, Devi Parikh, and Dhruv Batra. Grad-cam: Visual explanations from deep networks via gradient-based localization. In *ICCV*, pages 618–626. IEEE Computer Society, 2017. ISBN 978-1-5386-1032-9. URL http://dblp.uni-trier.de/db/conf/iccv/iccv2017.html#SelvarajuCDVPB17.

Han Shao, Omar Montasser, and Avrim Blum. A theory of pac learnability under transformation invariances. *Advances in Neural Information Processing Systems*, 35: 13989–14001, 2022.

Rulin Shao, Zhouxing Shi, Jinfeng Yi, Pin-Yu Chen, and Cho-Jui Hsieh. On the adversarial robustness of vision transformers. *arXiv preprint arXiv:2103.15670*, 2021.

Sho Sonoda, Isao Ishikawa, and Masahiro Ikeda. Ghosts in neural networks: Existence, structure and role of infinite-dimensional null space. *CoRR*, abs/2106.04770, 2021. URL https://arxiv.org/abs/2106.04770.

Andreas Peter Steiner, Alexander Kolesnikov, Xiaohua Zhai, Ross Wightman, Jakob Uszkoreit, and Lucas Beyer. How to train your vit? data, augmentation, and regularization in vision transformers. *Transactions on Machine Learning Research*, 2022. ISSN 2835-8856. URL https://openreview.net/forum?id=4nPswr1KcP.

Gilbert Strang. *Introduction to Linear Algebra, Fourth Edition*. Wellesley Cambridge Press, February 2009a. ISBN 0980232716. URL http://www.amazon.com/exec/obidos/redirect?tag=citeulike07-20&path=ASIN/0980232716.

Gilbert Strang. *Introduction to Linear Algebra*. Wellesley-Cambridge Press, Wellesley, MA, fourth edition, 2009b. ISBN 9780980232714 0980232716 9780980232721 0980232724 9788175968110 8175968117.

Haohan Wang, Songwei Ge, Zachary Lipton, and Eric P Xing. Learning robust global representations by penalizing local predictive power. In *Advances in Neural Information Processing Systems*, pages 10506–10518, 2019.

Haohan Wang, Zeyi Huang, Xindi Wu, and Eric Xing. Toward learning robust and invariant representations with alignment regularization and data augmentation. KDD '22, New York, NY, USA, 2022a. Association for Computing Machinery. ISBN 9781450393850. doi: 10.1145/3534678.3539438. URL https://doi.org/10.1145/3534678.3539438.

Jindong Wang, Cuiling Lan, Chang Liu, Yidong Ouyang, Tao Qin, Wang Lu, Yiqiang Chen, Wenjun Zeng, and Philip Yu. Generalizing to unseen domains: A survey on domain generalization. *IEEE Transactions on Knowledge and Data Engineering*, 2022b.

Shipeng Wang, Xiaorong Li, Jian Sun, and Zongben Xu. Training networks in null space of feature covariance for continual learning. In *Proceedings of the IEEE/CVF Conference on Computer Vision and Pattern Recognition (CVPR)*, pages 184–193, June 2021.

Raymond B. Wolfgang and Edward J. Delp. A watermark for digital images. *Proceedings of 3rd IEEE International Conference on Image Processing*, 3:219–222 vol.3, 1996.

Yao Xiao, Ziyi Tang, Pengxu Wei, Cong Liu, and Liang Lin. Masked images are counterfactual samples for robust fine-tuning. In *Proceedings of the IEEE/CVF Conference on Computer Vision and Pattern Recognition*, pages 20301–20310, 2023.

Catherine Yeh, Yida Chen, Aoyu Wu, Cynthia Chen, Fernanda Viégas, and Martin Wattenberg. Attentionviz: A global view of transformer attention. *arXiv preprint arXiv:2305.03210*, 2023.

Sangdoo Yun, Dongyoon Han, Seong Joon Oh, Sanghyuk Chun, Junsuk Choe, and Youngjoon Yoo. CutMix: Regularization strategy to train strong classifiers with localizable features. In *ICCV*, 2019.

Hongyang Zhang, Yaodong Yu, Jiantao Jiao, Eric Xing, Laurent El Ghaoui, and Michael Jordan. Theoretically principled trade-off between robustness and accuracy. In *ICML*, pages 7472–7482. PMLR, 2019.

Hongyi Zhang, Moustapha Cisse, Yann N. Dauphin, and David Lopez-Paz. mixup: Beyond empirical risk minimization. In *ICLR*, 2018. URL https://openreview.net/forum?id=r1Ddp1-Rb.

Xueyan Zou, Jianwei Yang, Hao Zhang, Feng Li, Linjie Li, Jianfeng Gao, and Yong Jae Lee. Segment everything everywhere all at once, 2023.

SUPPLEMENTARY MATERIAL

A NULLSPACE: PRIMER

For a linear mapping represented as f, where the domain is a vector space, the nullspace is a subspace that satisfies all the required axioms:

- The zero element of $\mathbb{R}^{1\times p}$, $\mathbf{0} \in \mathcal{N}$. This is true as $f(\mathbf{0}) = \mathbf{0}$.
- $\mathcal{N}$ is closed under vector addition. $\mathbf{u} + \mathbf{v} \in \mathcal{N}\ \forall \mathbf{u}, \mathbf{v} \in \mathcal{N}$. This is true as $f(\mathbf{u} + \mathbf{v}) = f(\mathbf{u}) + f(\mathbf{v}) = \mathbf{0}$.
- Closed under multiplication with a scalar. $c\mathbf{u} \in \mathcal{N}\ \forall\, c \in \mathbb{R}, \forall \mathbf{u} \in \mathcal{N}$. This is true as $f(c\mathbf{u}) = c(f(\mathbf{u})) = \mathbf{0}$.

A trivial nullspace, $\mathcal{N} = \{\mathbf{0}\}$, always exists for a linear mapping. An alternate way to interpret nullspace is to view it as a set of solutions to the homogeneous system of linear equations, implying that $\mathbf{0}$ is always a solution to the said equation. As the number of solutions to a system of linear equations can vary, the nullspace for a mapping can be trivial or nontrivial.

B PROOF OF PROPOSITION 1

Let d be the hidden dimension of the attention layer. $\mathbf{Q}_i, \mathbf{K}_i \in \mathbb{R}^{d\times d_k}$ where $d_k = d/h$. $\text{rank}(\mathbf{Q}_i\mathbf{K}_i^\top) \leq \text{rank}(\mathbf{K}_i^\top) \leq d_k$. Consider the sum of row spaces $S = \text{R}(\mathbf{Q}_1\mathbf{K}_1^\top) + \text{R}(\mathbf{Q}_2\mathbf{K}_2^\top) + \cdots + \text{R}(\mathbf{Q}_h\mathbf{K}_h^\top)$. S is a subspace of $\mathbb{R}^d$. For $i = 1, \ldots, h$, choose a basis for $\text{R}(\mathbf{Q}_i\mathbf{K}_i^\top)$, denoted as $B_i = \{\mathbf{b}_1, \cdots, \mathbf{b}_{n_i}\}$, $|B_i| = n_i \leq d_k$. Without loss of generality, let $\mathbf{r}_{m,k} \in B_m$.

$S = \text{span}(\bigcup_{i=1}^{h} B_i)$, so

$$\begin{aligned}\dim(S) &= \dim\left(\text{span}\left(\bigcup_{i=1}^{h} B_i\right)\right) = \dim\left(\text{span}\left(\left(\bigcup_{\substack{i=1\\ i\neq m}}^{h} B_i\right) \cup (B_m \setminus \{\mathbf{r}_{m,k}\})\right)\right) \\ &\leq \left|\left(\bigcup_{\substack{i=1\\ i\neq m}}^{h} B_i\right) \cup (B_m \setminus \{\mathbf{r}_{m,k}\})\right| \leq (h-1)d_k + (d_k - 1) = d - 1.\end{aligned} \tag{9}$$

So, $\exists \mathbf{w} \in \mathbb{R}^d, \mathbf{w} \neq \mathbf{0}$ and $\mathbf{w} \in S^\perp$. This means for $i = 1, \ldots, h, \mathbf{w} \in \left(\text{R}\left(\mathbf{Q}_i\mathbf{K}_i^\top\right)\right)^\perp, \mathbf{w} \in \text{N}\left(\mathbf{Q}_i\mathbf{K}_i^\top\right)$. By condition 2, $\text{N}(\mathbf{V}_i) \supseteq \text{N}(\mathbf{Q}_i\mathbf{K}_i^\top)$, so $\mathbf{w} \in \text{N}\left(\mathbf{Q}_i\mathbf{K}_i^\top\right) \cap \text{N}(\mathbf{V}_i^\top)$.

Then, we can choose $\mathbf{W}$ wherein each row is a multiple of $\mathbf{w}$. We have $\mathbf{W}\mathbf{V}_i = \mathbf{0}$, and for any input to the encoder $\mathbf{X} \in \mathbb{R}^{n\times d}$,

$$\mathbf{W}\mathbf{Q}_i\mathbf{K}_i^\top\mathbf{X}^\top + \mathbf{X}\mathbf{Q}_i\mathbf{K}_i^\top\mathbf{W}^\top + \mathbf{W}\mathbf{Q}_i\mathbf{K}_i^\top\mathbf{W}^\top = \mathbf{0}. \tag{10}$$

Consider the output of attention head,

$$\begin{aligned}\text{head}_i(\mathbf{X} + \mathbf{W}) &= \text{Softmax}\left(\frac{(\mathbf{X} + \mathbf{W})\,\mathbf{Q}_i\mathbf{K}_i^\top(\mathbf{X} + \mathbf{W})^\top}{\sqrt{d_k}}\right)(\mathbf{X} + \mathbf{W})\mathbf{V}_i \\ &= \text{Softmax}\left(\frac{\mathbf{X}\mathbf{Q}_i\mathbf{K}_i^\top\mathbf{X}^\top + \mathbf{W}\mathbf{Q}_i\mathbf{K}_i^\top\mathbf{X}^\top + \mathbf{X}\mathbf{Q}_i\mathbf{K}_i^\top\mathbf{W}^\top + \mathbf{W}\mathbf{Q}_i\mathbf{K}_i^\top\mathbf{W}^\top}{\sqrt{d_k}}\right)\mathbf{X}\mathbf{V}_i \\ &= \text{Softmax}\left(\frac{\mathbf{X}\mathbf{Q}_i\mathbf{K}_i^\top\mathbf{X}^\top}{\sqrt{d_k}}\right)\mathbf{X}\mathbf{V}_i = \text{head}_i(\mathbf{X}).\end{aligned} \tag{11}$$

Adding the noise $\mathbf{W}$ does not change the output of any attention head for arbitrary input $\mathbf{X}$, which completes our proof.

C ALGORITHM AND IMPLEMENTATION DETAILS

We present the algorithm of our data augmentation with nullspace noise in Algorithm 1.

Algorithm 1: Data augmentation with nullspace noise

Input: transformer model with patch embedding layer f_e, encoder f_ϕ and linear classifier f_ψ parameterized by e, ϕ, ψ respectively; training data $\mathcal{T}$; batch size B; sampling limit A; noise nullity threshold ϵ; noise learning rate η_v; model learning rate η_f; number of outer iterations K, noise training step T, model training step S

for $k = 0, \cdots, K-1$ **do**

  Sample initial noise $\mathbf{v} \sim \mathrm{U}(-\mathrm{lim}, \mathrm{lim})$

  for $t = 0, \cdots, T-1$ **do**

    Sample a minibatch $(\mathbf{X}, \mathbf{y}) \sim \mathcal{T}$

    Compute $\mathbf{U} \leftarrow f_e(\mathbf{X})$

    Compute logits $\mathbf{Z} \leftarrow f_\psi(f_\phi^0(\mathbf{U}))$, $\mathbf{Z}' \leftarrow f_\psi(f_\phi^0(\mathbf{U} + [\mathbf{v}]))$ `# "[v]" means broadcasting the noise v along the sample dimension`

    Compute $\delta \leftarrow \frac{1}{B}\sum_{i=1}^{B} \|\mathrm{Softmax}(\mathbf{z}_i') - \mathrm{Softmax}(\mathbf{z}_i)\|^2$ `# $\mathbf{z}_i$ is sample logit`

    if $\sigma < \epsilon$ **then**

      break

    end

    Calculate $\ell \leftarrow \frac{1}{B}\sum_{i=1}^{B} \|\mathbf{z}_i' - \mathbf{z}_i\|^2$

    Update $\mathbf{v} \leftarrow \mathbf{v} - \nabla_{\mathbf{v}} \ell$

  end

  for $s = 0, \cdots, S-1$ **do**

    Sample a minibatch $(\mathbf{X}, \mathbf{y}) \sim \mathcal{T}$

    Compute $\mathbf{U} \leftarrow f_e(\mathbf{X})$

    Compute logits $\mathbf{Z} \leftarrow f_\psi(f_\phi^0(\mathbf{U}))$, $\mathbf{Z}' \leftarrow f_\psi(f_\phi^0(\mathbf{U} + [\mathbf{v}]))$

    Compute loss $\mathcal{L} \leftarrow \frac{1}{B}\sum_{i=1}^{B}(\ell(\mathbf{z}_i, y_i) + \ell(\mathbf{z}_i', y_i))$, where ℓ is the cross-entropy loss

    Update model parameters $(\psi, \phi, e) \leftarrow (\psi, \phi, e) - \nabla_{(\psi,\phi,e)}\mathcal{L}$

  end

end

Output: model weight (ψ, ϕ, e)

Hyperparameters We fine-tuned the ViT model for $K = 20$ rounds in all settings. In each round, we initialized the noise with sampling limit $A = 3$, optimized it with learning rate $\eta_v = 0.1$ and set a threshold of $\epsilon = 0.03$. We empirically found that $T = 3000$ is enough to trigger early stopping so that the learned noise satisfies the ϵ threshold. We used $\eta_f = 10^{-5}$ to fine-tune the model for $S = 40$ iterations in each round. We set batch size $B = 128$, and slightly different from the vanilla SGD in Alg 1, we used the AdamW optimizer [Loshchilov and Hutter, 2019] and cosine learning rate scheduler with defualt hyperparameters for both the noise and the model training.

The original `ViT-B + DAT` model [Mao et al., 2022a] used the Exponential Moving Average (EMA) for evaluation[2], so we also used EMA to evaluate the performance of `ViT-B + DAT` fine-tuned with our method. For all the other settings, we used single model without ensemble for evaluation. We used $\epsilon = 1/255$ for the FGSM attack consistent with Mao et al. [2022a].

Computation time The experiments were conducted on a combination of A100, V100 GPUs and a 3090 GPU, depending on the availability. Although we only used about 10% of the ImageNet-1k [Deng et al., 2009] training data to fine-tune the model, the main computation time is on training the nullspace noise. One run of our experiment (20 rounds) takes the time roughly equivalent to 8 epochs of standard training on ImageNet-1k.

D CHANGE TREND OF THE NOISE INFLUENCE WITH THE FINE-TUNING STEPS

Beside the trend of noise norm and performance metrics in Fig. 4, we also keep track of the influence of the learned noise in terms of MSE probability (3.2) at every 80 steps of the model fine-tuning. As shown in Table 5, the noise influence is always lower than $\epsilon = 0.03$, which means early stopping is triggered and the model enters the ϵ region.

[2] `https://github.com/alibaba/easyrobust`

Table 5: MSE probability of the noise at different fine-tuning steps.

Fine-Tuning Step	40	120	160	280	360	440	520	600	680	760
MSE Probability	0.028	0.027	0.026	0.029	0.028	0.029	0.027	0.025	0.028	0.026

E WATERMARKING IMAGES

Watermarking as image, usually used to convey ownership information or verify content of the data, has been studied extensively [Wolfgang and Delp, 1996, Potdar et al., 2005, Al-Haj, 2007, Bhat et al., 2010]. A watermark can be either imperceptible or perceptible. and perceptible watermarking applies a noticeable marker to convey the protected nature of the data [Berghel, 1998]. In this section, we explore to utilize nullspace noise to apply a perceptible watermark on the image which does not alter the test-time forward process.

Figure 6 shows an example watermarking approach using the nullspace noise. Here, we emboss the ICML logo onto the natural images. The resulting modified image, attains the final predictions close to the original image. (100% match in the final output prediction and 10^{-4} difference in the predicted confidence value of the assigned class.)

Method details: With basis vectors of the nullspace, we can construct a watermark to be overlaid on the original image without affecting the output of the network. Given a source (user's image) and a target image (watermark), we simply need to estimate the scalar parameters corresponding to the basis vectors to satisfy $\sum_{i=0}^{i<m} \mathbf{e}_i \lambda_i = \mathbf{v}_\theta \approx \Delta \mathbf{x}_j$.

$\mathbf{e}_i$ are the basis vectors for the nullspace, λ_i are their corresponding scalar co-efficients which are to be determined and $\Delta \mathbf{x}_j$ is the changed required to convert j^{th} original image patch to j^{th} watermark image patch. This can be achieved through a constrained optimisation of the following form:

$$\min \|\Delta \mathbf{x}_j - \sum_{i=0}^{i<m} \mathbf{e}_i \lambda_i\|_p. \tag{12}$$

Here, Δx_j is the difference between the j^{th} channel of a source and target image and λ_i is the i^{th} nullspace basis vector of the patch embedding layer with the corresponding variable scalar e_i. We use a least-square solver to solve for the solution (Available readily with packages such as Numpy).

F TARGETED NULLSPACE NOISE

Due to the dimension reduction effect of the patch embedding layer in most ViTs, we can transfer an image to be visually similar to another image by human perception, without changing the output of the original image perceived by the model. This differs from adversarial examples in the following aspects:

1. The working direction to construct an adversarial example is the other way around. If the transformed image is to be considered an adversarial example, then our source becomes the target for adversarial training and our target becomes the source.
2. Generating targeted nullspace noise requires no backpropagation through the network
3. Not only does the final prediction on the transformed image matches the source image, the saliency maps also match. This is displayed in Fig. 7

Though the transformation is not perfect, we can spot that the transformed images are visually similar to target images rather than source images. Even with this difference in the input space, transformed images and source images are classified into the same category with roughly the same confidence.

As recent studies have shown, fooling can also be extended to the interpretability methods (XAI) Dombrowski et al. [2019] partially due the limitations exposed by recent studies [Dombrowski et al., 2019, Ghorbani et al., 2019, Heo et al., 2019]. However, in contrast to these works aiming to fool specific XAI method, our nullspace noise only depends on the model, not the XAI method.

Figure 6: **Watermark superposition using the nullspace basis vectors.**

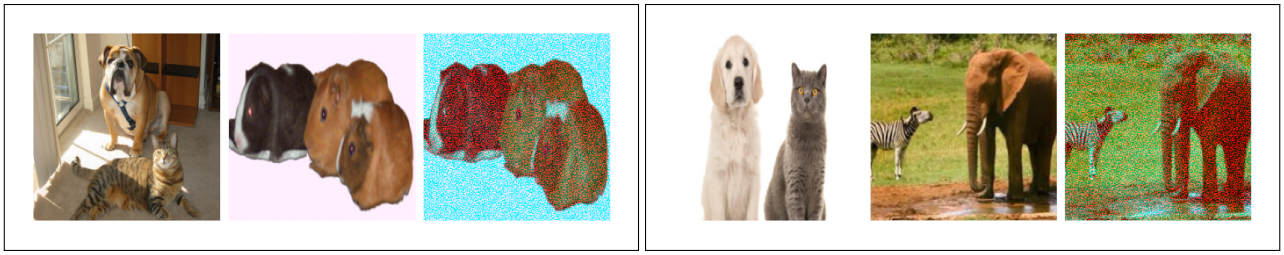

(a) Triplet of Source, target and transformed images

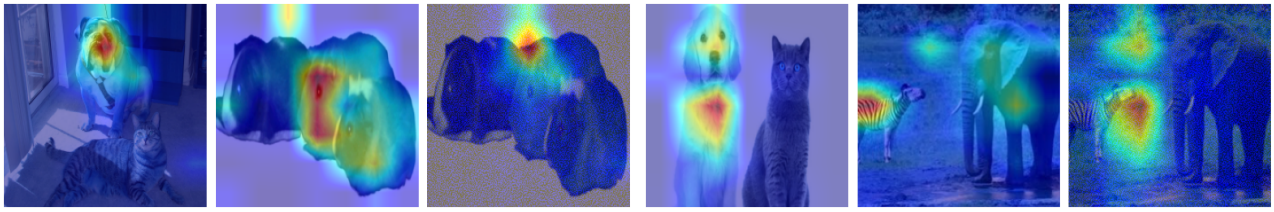

(b) Saliency maps for the corresponding images from the row above.

Figure 7: **Targeted nullspace noise.** Transformed images appear visually as target images but are interpreted as source images by the model. The equivalence between source and transformed images is not only in terms of the final predictions but also in the interpretability maps depicted in (b).

In Fig. 7(b), we show the interpretability maps as generated by LRP [Chefer et al., 2021]. From the figure, we can observe that the heatmaps generated by source and transformed images are identical whereas, the transformed image heatmaps substantially differ from target images'. Though only reported for LRP, we observed that a similar observation holds across different interpretability approaches. Here, we only presented the results on LRP, as in the context of ViTs, we found the heatmaps from other methods to be lacking (also pointed out by authors of LRP).

In Fig. 8 we show the saliency maps generated by different XAI methods. Even though the maps generated by methods other than LRP are poor (hard to interpret), we see that the source and transformed respond similarly to these methods.

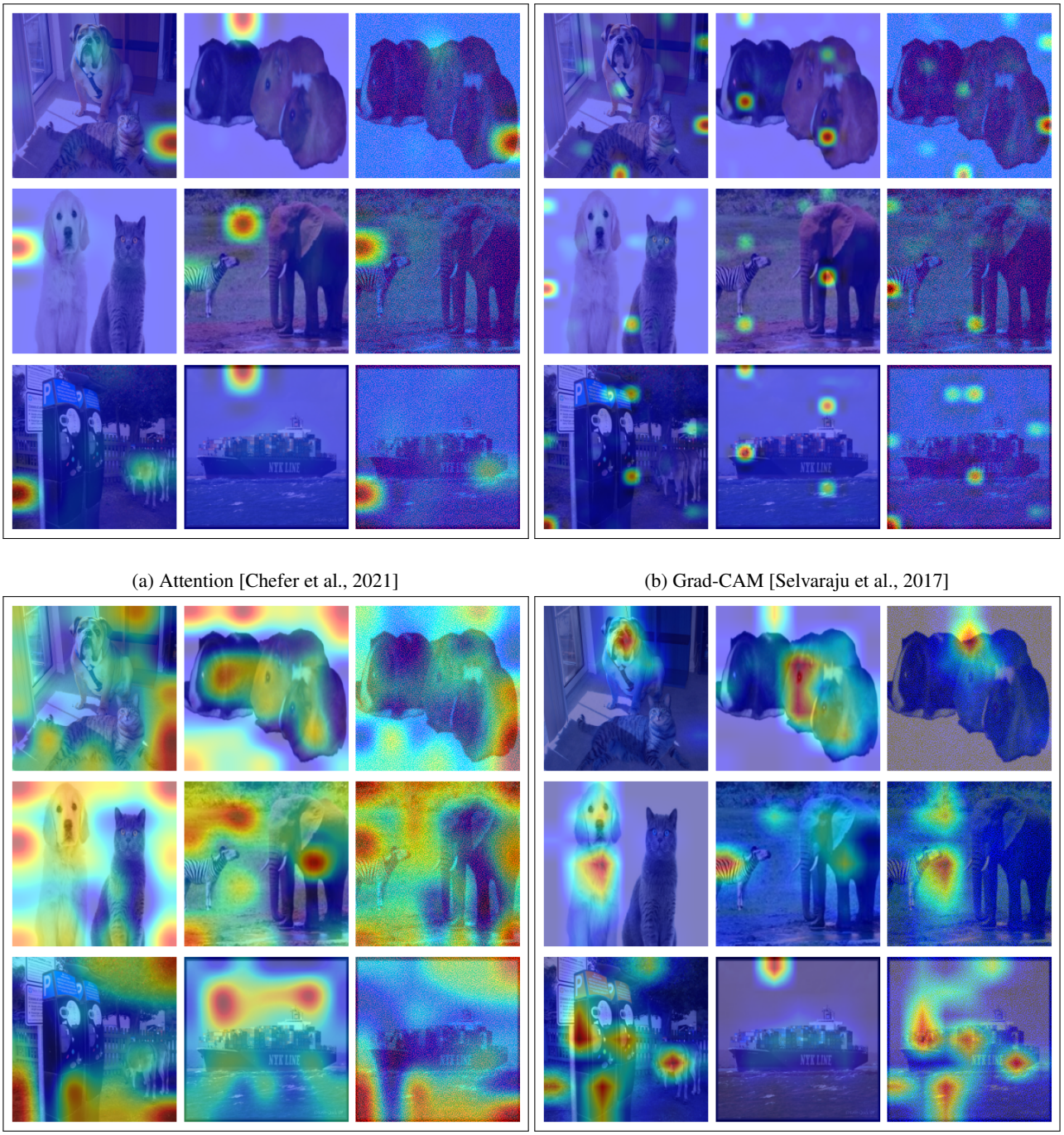

(a) Attention [Chefer et al., 2021]

(b) Grad-CAM [Selvaraju et al., 2017]

(c) Rollout [Abnar and Zuidema, 2020]

(d) LRP [Chefer et al., 2021]

Figure 8: **Interpretability maps generated via different methods for (source, target, transformed) images.**